Journal of Biomechanics 89 (2019) 78–84

Contents lists available at ScienceDirect

Journal of Biomechanics

journal homepage: www.elsevier.com/locate/jbiomech
www.JBiomech.com

Flow over a ski jumper in flight: Prediction of the aerodynamic force and flight posture with higher lift-to-drag ratio

Woojin Kim [a], Hansol Lee [b], Jungil Lee [c], Daehan Jung [d], Haecheon Choi [a,b,*]

[a] Institute of Advanced Machines and Design, Seoul National University, Seoul 08826, Republic of Korea
[b] Department of Mechanical & Aerospace Engineering, Seoul National University, Seoul 08826, Republic of Korea
[c] Department of Mechanical Engineering, Ajou University, Suwon 16499, Republic of Korea
[d] Department of Mechanical Engineering, Korea Air Force Academy, Cheongju 28187, Republic of Korea

ARTICLE INFO

Article history:
Accepted 12 April 2019

Keywords:
Ski jumping
Flight posture
Lift-to-drag ratio
Large eddy simulation
Simple geometric model

ABSTRACT

Large eddy simulations (LESs) are performed to study the flow characteristics around two flight posture models of ski jumping. These models are constructed by three-dimensionally scanning two national-team ski jumpers taking flight postures. The drag and lift forces on each component of a ski jumper and skis (head with helmet and goggle, body, arms, legs and skis) and their lift-to-drag ratios are obtained. For the two posture models, the drag forces on the body, legs and skis are larger than those on the arms and head with helmet and goggle, but the lift forces on the body and skis are larger than their drag forces, resulting in high lift-to-drag ratios on the body and skis and low lift-to-drag ratio on the legs. We construct simple geometric models, such as the circular cylinder, sphere and thin rectangular plate, predicting the drag and lift forces on each component of a ski jumper and skis, and validate them with those obtained from LES. Using these geometric models, we perform a parametric study on the position angles of flight posture for higher total lift-to-drag ratio. The flight postures obtained increase the total lift-to-drag ratios by 35% and 21% from those of two base postures, respectively. Finally, LESs are performed for the postures obtained and show the increases in the total lift-to-drag ratios by 21% and 16%, respectively, indicating the adequacy of using the simple geometric models for finding a flight posture of ski jumping having a higher lift-to-drag ratio at low cost.

1. Introduction

Ski jumping is a winter sport and composed of in-run, take-off, flight, and landing phases. The score of ski jumping is evaluated by the distance jumped and style score given by five judges. The flight distance is determined by the weight of a ski jumper and skis, aerodynamic forces during flight, and initial flight velocity, where the initial flight velocity is determined from the approach and take-off jump velocities and posture transition from in-run to flight (body extension and raising ski head) (Schmölzer and Müller, 2005; Schwameder, 2008; Yamamoto et al., 2016). The aerodynamic force is affected by the flight posture of a ski jumper. Therefore, ski jumpers put significant amounts of efforts to find their own optimal flight postures. However, it is not straightforward to find optimal postures during the flight phase by ski jumpers themselves because of many factors determining the flight posture and very short flight time. For example, one of the important factors is the ski-opening angle. The V style, pioneered by Jan Boklöv (Sweden) in 1985, replaced the parallel style because it improved the aerodynamic performance and increased the flight distance by allowing a ski jumper to lean forward (Müller, 2009). On the other hand, the H style with very small ski opening angle and wide spacing between skis becomes popular. However, the effect of these different styles on the aerodynamic performance has not been fully understood.

Flow around a ski jumper during flight has been studied experimentally and numerically. Müller et al. (1995) investigated the effect of the V-style flight posture for the first time and analyzed the first jump in history (over more than 200 m) achieved during the 1994 Ski Flying World Championships in Plancia, Slovenia. Müller et al. (1996) conducted large-scale wind tunnel experiments to measure the drag and lift areas on ski jumpers for three attack angles, calculated the flight trajectory, and investigated the effects of body mass, approach and take-off jump velocities, and wind direction. They found that a light ski jumper moved farther with a noticeably lower velocity, high approach and take-off jump velocities increased the flight distance, and the wind angle

* Corresponding author.
E-mail address: choi@snu.ac.kr (H. Choi).

https://doi.org/10.1016/j.jbiomech.2019.04.022
0021-9290/

relative to the horizontal direction in the range of 36–216° increased the flight distance with a relatively lower landing velocity. They also showed that the drag and lift areas were decreased by about 54% and 56%, respectively, with an almost same lift-to-drag ratio, as the ski-opening angle decreased from 35° to 0°. Schmölzer and Müller (2002) recorded a series of flight postures of the best ski jumpers during 1999/2000 World Cup competitions in Villach through field studies, measured the attack angle and position angles (body-ski angle, hip angle, and ski-opening angle), performed the least-square fits for the attack angle, body-ski angle, and hip angle as a function of flight time, and conducted large-scale wind tunnel experiments for two flight posture models with different height and ski length at the measured angles (derived from field studies during the competitions) to obtain their drag and lift areas. They obtained increases of lift-to-drag ratio and lift, and a decrease of drag with decreasing hip angle from 180° to 170°. As the angle of attack decreased from 40° to 30° or the body-ski angle decreased from 15° to 1°, the lift-to-drag ratio increased but both the drag and lift decreased. Seo et al. (2004) optimized the flight distance by controlling the ski-opening and body-ski angles during flight for a simple flight posture model, and increased the flight distance from 131 m to 139 m at the body-ski angle of 7° by changing the ski-opening angle from 25° to around 26°. They found that the control of the ski-opening angle was more important for increasing the flight distance than that of the body-ski angle. Meile et al. (2006) obtained the drag and lift areas and pitching moment on a flight posture model through wind-tunnel experiments for various attack, body-ski, hip, head, shoulder abduction, and ski-opening angles. They found that the drag area continuously increased with the attack and body-ski angles, while many local maxima of the lift area existed and the lift area maintained a maximum near the sum of the attack and body-ski angles of about 50°. Jung et al. (2014) performed an optimization study for the flight distance by controlling the attack and body-ski angles during flight with constraints on the upper and lower limits of the attack and body-ski angles, respectively, and increased the flight distance from 113.8 m (Schmölzer and Müller, 2002) to 125.9 m. Yamanobe et al. (2016) investigated the effects of the upper limb position of a woman mannequin model on the aerodynamic forces. They concluded that the shoulder abduction angle should be smaller to obtain larger lift-to-drag ratio and the palm of the hand should be pointing in the flight direction to gain higher lift force. Jung et al. (2018) developed a new wind-compensation approach for the flight distance to more accurately compensate the effects of the wind deviating from the tangent to the flight path. However, as Schmölzer and Müller (2005) showed, different athletes differ markedly in their flight style, which indicates that the optimal posture of a simple model may be quite different from that of a real ski jumper.

Lee et al. (2012) conducted Reynolds-averaged Navier-Stokes (RANS) simulations on a simple model, and increased the lift-to-drag ratio by 28.8% through the optimization of the attack angle (from 30° to 12°) and body-ski angle (from 26° to 20°) at the hip angle of 160° and ski-opening angle of 35°. Gardan et al. (2017) conducted RANS simulations for a three-dimensional (3D) ski jumper model constructed based on laser-scanned helmet and skis and anthropological data for a ski jumper. They obtained maximum lift-to-drag ratio and minimum drag and lift coefficients at the attack angle of $\alpha = 14°$ in the range of $14° \leq \alpha \leq 44°$. However, Meile et al. (2006) showed the deviations of 20% in the drag coefficient and 11–34% in the lift coefficient between RANS simulations and wind-tunnel experiments for a simple model. Therefore, a high-fidelity simulation is required to accurately predict the flow around a flight posture of ski jumping.

So far, many of previous studies have adopted a simple ski jumper model for wind-tunnel tests and numerical simulations, and investigated the effects of the attack angle and position angles on the aerodynamic performance and flight distance. However, ski jumpers have different flight postures and may have different effects from those angles. Therefore, the objectives of the present study are to obtain the aerodynamic forces on typical flight postures by conducting large eddy simulations (LESs), and to develop simple geometric models of predicting them on the components of the postures for suggesting better flight postures.

2. Methods

Two flight postures of ski jumping are constructed by three-dimensionally scanning those of two national-team ski jumpers, as shown in Fig. 1. The center lines of body, arms, legs, and skis are used to determine their attack angles (α), roll angles (ϕ) and yaw angles (λ), and these flight posture parameters for jumpers 1 and 2 are given in Table 1. The attack angle of skis, $\alpha_{Ski\ body}$, is known to be an important parameter to determine the flight distance and it has been observed to increase continuously from 26° to 39° during the flight (measured for the best ten jumpers in the 19th Winter Olympic Games by Schmölzer and Müller, 2005). Since we could not measure this angle of attack for the present posture models, we fix the attack angle of skis at $\alpha_{Ski\ body} = 30°$ for jumpers 1 and 2 which is near the time-averaged angle of attack of 28.5° during the flight (Schmölzer and Müller, 2005). The ski length (l), minimum ski spacing (s/l), and frontal (A_f) and planform (A_p) areas are 2.43 m, 0.08, 0.622 m^2 and 1.020 m^2 for jumper 1, and 2.54 m, 0.10, 0.755 m^2 and 1.183 m^2 for jumper 2, respectively.

We perform LESs of flows over two flight postures, respectively. The numerical details are given in the Supplementary materials. The Reynolds numbers considered are $\mathrm{Re} = \rho U l/\mu = 540{,}000$ for jumper 1 and 564,000 for jumper 2 due to slightly different ski lengths of jumpers 1 and 2, where ρ and μ are the fluid density and viscosity, respectively, and U is the flight speed. The present Reynolds numbers are much lower than those in field studies, but still provide meaningful interpretation on the force coefficients (see Supplementary materials). Note that the postures under consideration include helmet and goggle, but the interaction between air and soft suit is not considered in our numerical simulation. The numbers of grid points are 801 (x) × 685 (y) × 689 (z) (about 378 million grid points) for jumper 1 and 849 (x) × 697 (y) × 689 (z) (about 407 million grid points) for jumper 2 (see Supplementary materials for the detail).

The results from LES include the flow characteristics around and the drag and lift forces on the posture models. Especially, LES provides the drag and lift forces on each component of the posture models such as the head with helmet and goggle, body, arms, legs, and skis. With this information, we develop simple geometric models to predict the drag and lift forces on the components of the posture models. These geometric models are used to obtain better flight postures having higher aerodynamic performances with very low cost. Finally, LES is performed for the postures suggested from simple geometric models to compare the drag and lift forces with those from the simple geometric models.

3. Results

3.1. Aerodynamic forces

Table 2 shows the time-averaged drag area ($\bar{C}_D A_p$), lift area ($\bar{C}_L A_p$), and lift-to-drag ratio ($\bar{L}/\bar{D}$) for jumpers 1 and 2, together with those of jumper 1 from a laboratory experiment by Bang et al. (2015). Here, $C_D = D/\left(0.5\rho U^2 A_p\right)$ and $C_L = L/\left(0.5\rho U^2 A_p\right)$

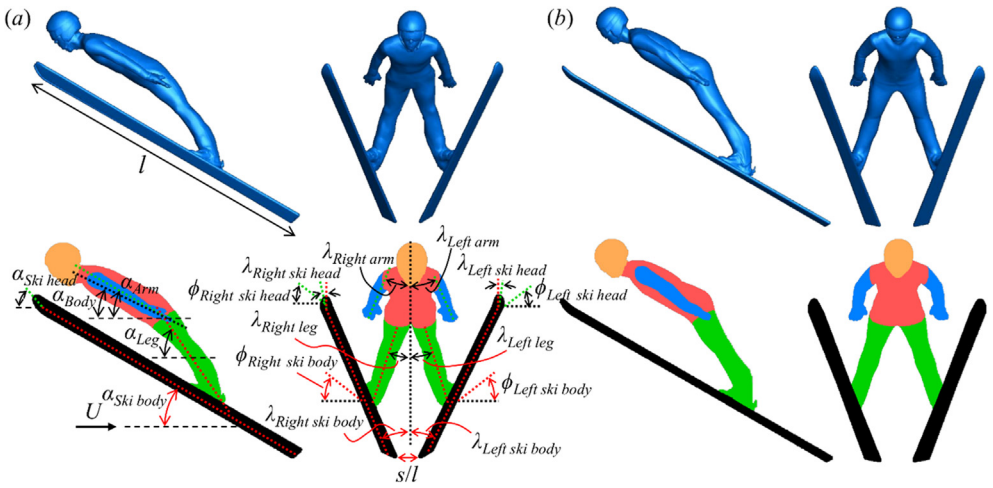

Fig. 1. Three-dimensionally scanned flight postures: (a) jumper 1; (b) jumper 2. For modelling purpose, the aerodynamic forces on each jumper and skis are decomposed into those on the jumper's head with helmet and goggle, body, legs, arms, and skis that are represented with orange, red, green, blue, and black colors, respectively. Here, U is the flight speed, l is the ski length, s is the minimum spacing between right and left skis, α_i's are the attack angles, ϕ_i's are the roll angles, and λ_i's are the yaw angles. (For interpretation of the references to colour in this figure legend, the reader is referred to the web version of this article.)

Table 1
Attack angles (α), yaw angles (λ), and roll angles (ϕ) for left and right skis, left and right legs, left and right arms, and body for jumpers 1 and 2. Note that the angles of left and right components are not necessarily same because the postures are not in a perfect reflection symmetry. Here, the attack angle $\alpha_{Ski\ body}$ (Fig. 1) is fixed at 30° which is one of many attack angles observed during flight.

	Left ski body		Right ski body		Left ski head		Right ski head		Left leg		Right leg		Left arm		Right arm		Body	
Jumper	1	2	1	2	1	2	1	2	1	2	1	2	1	2	1	2	1	2
α (°)	30	30	30	30	46	49	46	49	53	57	53	57	28	35	25	35	24	29
λ (°)	14	11	12	11	1	4	0	4	13	15	14	15	14	18	15	18	0	0
ϕ (°)	40	18	34	18	42	20	36	20	0	0	0	0	0	0	0	0	0	0

Table 2
Time-averaged drag areas, lift areas, and lift-to-drag ratios obtained from LES and experiment for jumpers 1 and 2.

		$\bar{C}_D A_p$	$\bar{C}_L A_p$	$\bar{L}/\bar{D}$
Jumper 1	LES (present)	0.410	0.556	1.357
	Experiment (Bang et al. 2015)	0.415	0.581	1.383
Jumper 2	LES (present)	0.543	0.673	1.240

are the drag and lift coefficients, respectively, D and L are the drag and lift forces, respectively, A_p is the planform area, and an overbar denotes the time averaging. The drag area, lift area, and lift-to-drag ratio of jumper 1 obtained from present LES agree well with those from an experiment. The drag and lift areas of jumper 2 are 32.4% and 21.0% higher than those of jumper 1, but the lift-to-drag ratio of jumper 2 is 8.6% lower than that of jumper 1.

A benefit of numerical simulation is that the force on each component of the jumper and skis can be obtained. Fig. 2 shows the time-averaged drag area, lift area, and lift-to-drag ratio of head with helmet and goggle (called head hereafter), body, arms, legs, and skis for two jumpers. For jumper 1, the drag force is largest on legs and then on body, but it is largest on the body and then legs and skis for jumper 2. The drags on head and arms are very small compared to those on other parts. The lift force is largest on body for jumper 1, but on skis for jumper 2. The lift forces on head, arms and legs are much smaller than those on body and skis. The lift-to-drag ratio is large on arms, skis and body, but those on legs and head are small. The high lift-to-drag ratio of arms does not actually contribute to the total lift-to-drag ratio because the forces on arms are too small. Since the portions of the drag and lift forces of head are less than 9% and those of arms are less than 13%, it is important to modify the postures of legs, skis and body, in order to improve the overall aerodynamic performance.

3.2. Modeling the aerodynamic forces on each component of a jumper and skis

Owing to many parameters determining the posture of a jumper and skis (Table 1), an immense amount of effort is required to find an optimal posture of a jumper by numerical simulation and experiment. For example, an LES for one posture requires a CPU time of about two weeks with four CPU cores of the Intel i7-3820. Therefore, in this section, we suggest simple geometric models for prediction of forces on each component of jumper and skis at low cost. With these models, it should be much easier and faster to find a better posture providing higher lift-to-drag ratio.

Fig. 3 shows simple geometric models for the components of jumper and skis. As shown, we model head as a sphere, body as an inclined thin rectangular plate, arms and legs as circular cylinders, and ski body and head as inclined thin rectangular plates. In our models, we neglect the friction force because the force due to the pressure difference is much larger than the friction force for the bluff bodies. Then, the aerodynamic force on each component is perpendicular to the model surface. The force coefficients normal to the sphere, circular cylinder, and inclined thin rectangular plate can be found in Blevins (1984), in which the force coefficients normal to the sphere and cylinder are given as a function of the Reynolds number, and the force coefficient normal to an inclined thin

rectangular plate is given as a function of the inclined angle and the aspect ratio of the plate (Table 3). Therefore, we formulate the forces on each component according to the data provided in Blevins (1984).

The centerline ($\vec{l}_c$) and normal ($\vec{l}_n$) unit vectors of each component in Cartesian coordinates can be expressed with the attack (α), yaw (λ) and roll (ϕ) angles as follows:

$$\vec{l}_c = (l_{cx}, l_{cy}, l_{cz}) = (-\cos\lambda\cos\alpha,\ \cos\lambda\sin\alpha,\ \sin\lambda), \tag{1}$$

$$\begin{aligned}\vec{l}_n &= (l_{nx}, l_{ny}, l_{nz}) \\ &= (\cos\phi\sin\alpha - \sin\lambda\sin\phi\cos\alpha,\ \cos\phi\cos\alpha + \sin\lambda\sin\phi\sin\alpha,\ -\cos\lambda\sin\phi).\end{aligned} \tag{2}$$

With these centerline and normal vectors, total drag and lift areas are obtained as

$$\begin{aligned}(C_D A_p, C_L A_p) = {} & (C_N)_{Head}(A_N)_{Head}(l_{nx}, l_{ny})_{Head} + (C_N)_{Body}(A_N)_{Body}(l_{nx}, l_{ny})_{Body} \\ & + (C_N)_{Left\ arm}(A_N)_{Left\ arm}\left\{\left|\vec{i}_U - \left(\vec{i}_U\cdot\vec{l}_c\right)\vec{l}_c\right|\right\}^2_{Left\ arm}(l_{nx}, l_{ny})_{Left\ arm} \\ & + (C_N)_{Right\ arm}(A_N)_{Right\ arm}\left\{\left|\vec{i}_U - \left(\vec{i}_U\cdot\vec{l}_c\right)\vec{l}_c\right|\right\}^2_{Right\ arm}(l_{nx}, l_{ny})_{Right\ arm} \\ & + (C_N)_{Left\ leg}(A_N)_{Left\ leg}\left\{\left|\vec{i}_U - \left(\vec{i}_U\cdot\vec{l}_c\right)\vec{l}_c\right|\right\}^2_{Left\ leg}(l_{nx}, l_{ny})_{Left\ leg} \\ & + (C_N)_{Right\ leg}(A_N)_{Right\ leg}\left\{\left|\vec{i}_U - \left(\vec{i}_U\cdot\vec{l}_c\right)\vec{l}_c\right|\right\}^2_{Right\ leg}(l_{nx}, l_{ny})_{Right\ leg} \\ & + (C_N)_{Left\ ski\ body}(A_N)_{Left\ ski\ body}\left\{\left|\left(\vec{i}_U\cdot\vec{l}_c\right)\vec{l}_c + \left(\vec{i}_U\cdot\vec{l}_n\right)\vec{l}_n\right|\right\}^2_{Left\ ski\ body}(l_{nx}, l_{ny})_{Left\ ski\ body} \\ & + (C_N)_{Right\ ski\ body}(A_N)_{Right\ ski\ body}\left\{\left|\left(\vec{i}_U\cdot\vec{l}_c\right)\vec{l}_c + \left(\vec{i}_U\cdot\vec{l}_n\right)\vec{l}_n\right|\right\}^2_{Right\ ski\ body}(l_{nx}, l_{ny})_{Right\ ski\ body} \\ & + (C_N)_{Left\ ski\ head}(A_N)_{Left\ ski\ head}\left\{\left|\left(\vec{i}_U\cdot\vec{l}_c\right)\vec{l}_c + \left(\vec{i}_U\cdot\vec{l}_n\right)\vec{l}_n\right|\right\}^2_{Left\ ski\ head}(l_{nx}, l_{ny})_{Left\ ski\ head} \\ & + (C_N)_{Right\ ski\ head}(A_N)_{Right\ ski\ head}\left\{\left|\left(\vec{i}_U\cdot\vec{l}_c\right)\vec{l}_c + \left(\vec{i}_U\cdot\vec{l}_n\right)\vec{l}_n\right|\right\}^2_{Right\ ski\ head}(l_{nx}, l_{ny})_{Right\ ski\ head},\end{aligned} \tag{3}$$

where $\vec{i}_U = (1,0,0)$ is the unit vector of freestream velocity, $(A_N)_{Head} = \pi(D_{Head})^2/4$, $D_{Head} = (6V_{Head}/\pi)^{1/3}$, V_{Head} is the volume of head, $(A_N)_{Body} = w_B l_B$, w_B and l_B are the width and length of body, $(A_N)_{Arm} = l_{Arm}D_{Arm}$, $D_{Arm} = (4V_{Arm}/\pi l_{Arm})^{0.5}$, l_{Arm} is the length of arm, V_{Arm} is the volume of arm, $(A_N)_{Leg} = l_{Leg}D_{Leg}$, $D_{Leg} = (4V_{Leg}/\pi l_{Leg})^{0.5}$, l_{Leg} is the length of leg, V_{Leg} is the volume of leg, $(A_N)_{Ski\ body} = w_{Sb}l_{Sb}$, w_{Sb} and l_{Sb} are the width and length of ski body, $(A_N)_{Ski\ head} = V_{Sh}/h_{Sh}$ ($\equiv w_{Sh}l_{Sh}$), V_{Sh} and h_{Sh} are the volume and thickness of ski head, and w_{Sh} ($=w_{Sb}$) and l_{Sh} are the width and length of ski head, respectively. The force coefficients on the head (sphere), arms (cylinders) and legs (cylinders) are obtained from Table 3 using linear interpolation, and the force coefficients on the ski and body (inclined thin rectangular plates) are obtained from Table 3 using bilinear interpolation or extrapolation (see Supplementary materials for the detail). Note that we neglect the change in the force coefficient due to connection of two geometric models.

Fig. 4 shows the comparison of the drag and lift force areas on each component from LES and simple geometric models. The drag and lift areas predicted from the present geometric models agree well with those from LES: i.e., the drag and lift forces are largest on the legs and body, respectively, for jumper 1, and, for jumper 2, the drag force is large on the body, legs and skis but the lift force is large on the body and skis.

3.3. Flight postures suggested by the present geometric models

Flight postures are searched for, based on the present geometric models, to increase the lift-to-drag ratio with a constraint that total lift force should not be smaller than that of the base posture. We varied the attack angles of legs, yaw angles of legs and skis, and roll angles of skis by fixing the attack angle of ski body ($\alpha_{Ski\ body} = 30°$) and the postures of head, arms, and body. We did not use any special optimization method but calculated the drag and lift forces for all the cases in the ranges of $30° \le \alpha_{Leg}$ ($=\alpha_{Right\ leg} = \alpha_{Left\ leg}$) $\le 60°$, $0° \le \lambda_{Leg}$ ($=\lambda_{Right\ leg} = \lambda_{Left\ leg}$), $\lambda_{Left\ ski\ body}$, $\lambda_{Right\ ski\ body}$, $\phi_{Left\ ski\ body}$, $\phi_{Right\ ski\ body} \le 40°$ by increments of 1° for each angle, respectively. Note that we did not assume a symmetry for the left and right ski angles, because the scanned shapes of left and right skis were not perfectly reflection symmetric. Therefore, the cases considered were more than 4 billion, but the computation took less than one minute with one CPU core of the Intel i7-3820.

Fig. 5 shows the contours of the total lift-to-drag ratio obtained for each α_{Leg} and λ_{Leg} using the present geometric models. The optimal posture of legs and skis for jumper 1 (denoted as blue triangle in this figure) is $\alpha_{Leg} = 30°$, $\lambda_{Leg} = 13°$, $\phi_{Right\ ski\ body} = 29°$, $\lambda_{Right\ ski\ body} = 17°$, $\phi_{Left\ ski\ body} = 28°$, $\lambda_{Left\ ski\ body} = 17°$, and that for jumper 2 is $\alpha_{Leg} = 30°$, $\lambda_{Leg} = 13°$, $\phi_{Right\ ski\ body} = 12°$, $\lambda_{Right\ ski\ body} = 16°$, $\phi_{Left\ ski\ body} = 11°$, $\lambda_{Left\ ski\ body} = 16°$. The 1° difference in the roll angles of left and right ski bodies is due to asymmetric ski and body shapes, but this difference is negligible. The total lift-to-drag ratios of the postures are increased by about 35% and 21% for jumpers 1 and 2, respectively, compared to those of the base postures.

To confirm the results from the present geometric models, we performed another LES on the postures shown in Fig. 5. The total lift forces are increased by 4% and 2% for jumpers 1 and 2, respectively, and the total drag forces are decreased by 14% and 12%, respectively. The total lift-to-drag ratios of the postures obtained from LES for jumpers 1 and 2 are increased by about 21% and

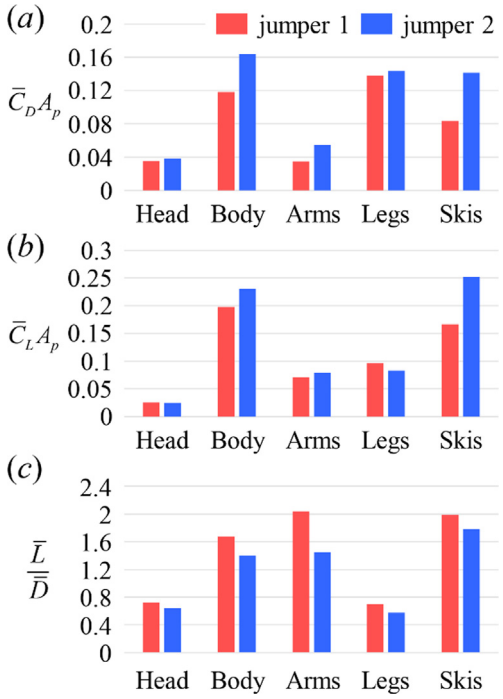

Fig. 2. Time-averaged drag area, lift area, and lift-to-drag ratio of head, body, arms, legs, and skis for jumpers 1 and 2; (*a*) $\bar{C}_D A_p$; (*b*) $\bar{C}_L A_p$; (*c*) $\bar{L}/\bar{D}$. Here, C_D (=D/($0.5\rho U^2 A_p$)) and C_L (=L/($0.5\rho U^2 A_p$)) are the drag and lift coefficients, respectively, L and D are the lift and drag forces, respectively, ρ is the fluid density, U is the flight speed, and A_p is the overall planform area.

16%, respectively, from those of the base postures. Although the amounts of the lift-to-drag ratio from the present geometric models are not the same as those from LES, they can still provide better flight postures with a low amount of efforts.

4. Discussion

In the present study, large eddy simulations were conducted for flows around two flight postures, and provided the drag and lift forces and lift-to-drag ratio on them. The simulation results indicated that flow massively separates from head, body, arms, legs and skis due to high attack angles to these components (α_i = 29–57°), which significantly decreases the lift force and increases the drag force. The details of flow structures are given in Supplementary materials.

Let us now discuss the prediction capability of simple geometric models. For the base postures, the differences in the total drag and lift areas predicted by simple geometric models and calculated by LES were 25% and 21% for jumper 1, respectively, and 7% and 4% for jumper 2, respectively. These amounts of differences are comparable to those from RANS simulation and experiment according to Meile et al. (2006) (20% for the drag area and 11–34% for the lift area), indicating that the present geometric models perform well while using very low computational time. Note, however, that even a few percentage difference in the drag and lift areas may cause a significant amount of changes in the flight distance (Müller, 2009). Thus, the present geometric models may be used as a design tool for suggesting better flight postures for higher lift-to-drag ratios.

The present geometric models provided flight postures of higher lift-to-drag ratios, in which the attack angles of legs were decreased from 53° (jumper 1) and 57° (jumper 2) to 30° at the attack angle of body of 24° (jumper 1) and 29° (jumper 2). It means that the hip angles increased from 151° to 174° (jumper 1) and from 152° to 179° (jumper 2), and the body-ski angles decreased from 11° to 1° (jumper 1) and from 17° to 5° (jumper 2) for higher lift-to-drag ratio. This is consistent with those of previous studies. That is, Meile et al. (2006) achieved maximum lift-to-drag ratio at the hip angle of 170° in the range of 150° – 180°. On the other hand, Schmölzer and Müller (2002) showed that the drag and lift areas were increased with almost constant lift-to-drag ratio as the hip angle increased from 150° to 170°. On the other hand, Müller

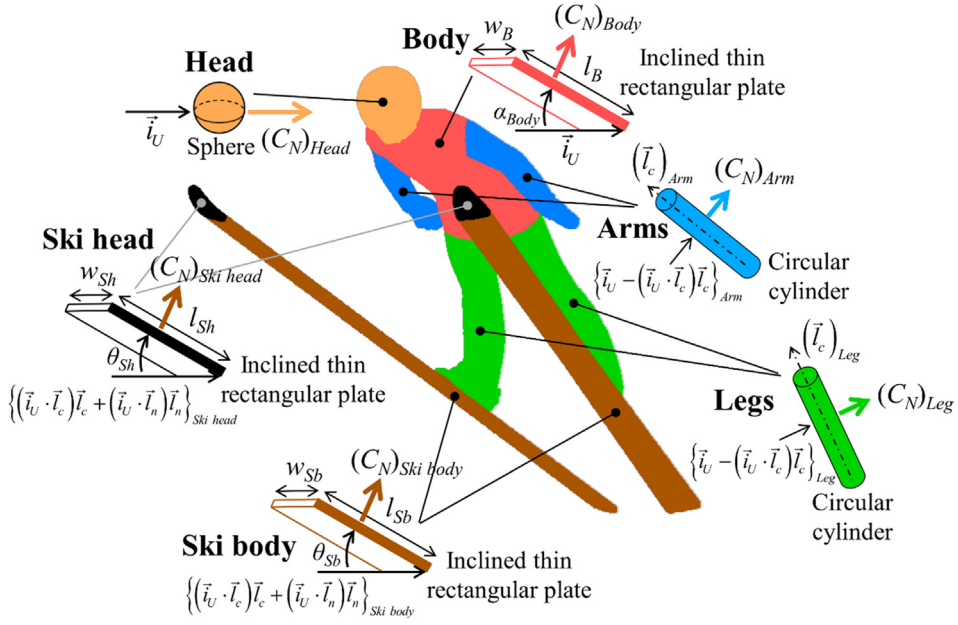

Fig. 3. Simple geometric models of predicting the drag and lift areas of the components of jumper and skis. Head, arms, body, legs, and skis are modeled as a sphere, circular cylinder, inclined thin rectangular plate, circular cylinder, and inclined thin rectangular plate, respectively, and the normal force coefficients (C_N) for these simple geometries are obtained from Blevins (1984). Here, $\vec{i}_U = (1,0,0)$ is the unit vector of the free-stream velocity, the inclined angle of ski body or head (θ_{Sb} or θ_{Sh}) is the angle between $(\vec{l}_c)_{Ski\ body\ or\ Ski\ head}$ and $\{(\vec{i}_U \cdot \vec{l}_c)\vec{l}_c + (\vec{i}_U \cdot \vec{l}_n)\vec{l}_n\}_{Ski\ body\ or\ Ski\ head}$, and $\vec{l}_c$ and $\vec{l}_n$ are its centerline and normal unit vectors, respectively.

Table 3
Force coefficients (C_N) normal to the sphere and circular cylinder with the Reynolds number, and to an inclined thin rectangular plate with the aspect ratio (w_p/l_p) and the inclined angle (θ_p) (Blevins, 1984). Here, w_p and l_p are the width and length of the plate, respectively, and θ_p is the inclined angle. Note that we neglect the change in the force coefficients due to connection of two geometric models.

	Re									
	10^2	5×10^2	10^3	5×10^3	10^4	5×10^4	10^5	5×10^5	10^6	5×10^6
Sphere	1.0	–	0.41	–	0.39	–	0.52	–	0.12	0.18
Circular cylinder	1.19	1.01	0.93	0.87	1.12	0.55	0.13	0.42	–	–

Inclined thin rectangular plate	w_p/l_p					
θ_p (°)	1/6	1/3	1.0	1.5	2	3
0	0	0	0	0	0	0
10	0.174	0.2442	0.399	0.3959	0.495	0.555
20	0.464	0.5883	0.8715	0.856	0.99	0.8436
30	0.7772	0.9657	1.281	0.856	0.803	0.8436
40	1.0672	1.332	1.47	0.9095	0.858	0.9435
50	1.2064	1.2543	1.1025	0.963	0.913	0.999
60	1.218	1.1655	1.0815	1.0058	0.99	1.0434
70	1.2064	1.1544	1.071	1.0379	1.045	1.0767
80	1.1948	1.1322	1.0605	1.0486	1.067	1.0878
90	1.16	1.11	1.05	1.07	1.1	1.11

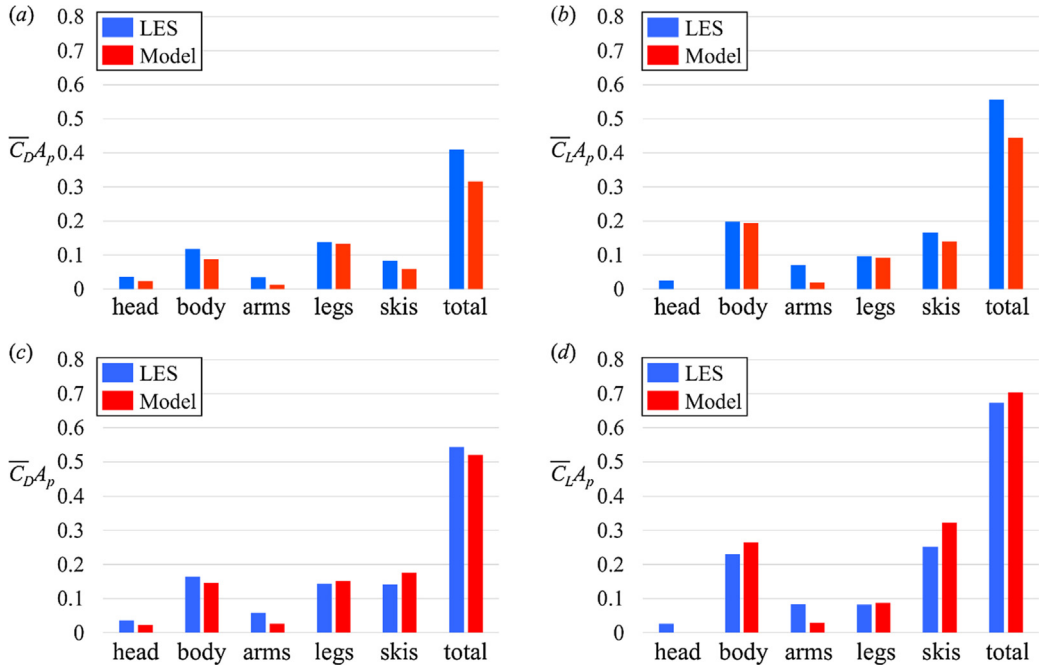

Fig. 4. Comparison of drag and lift areas on head, body, arms, legs, and skis and their sums obtained from LES and present geometric models: (a) drag area and (b) lift area for jumper 1, and (c) drag area and (d) lift area for jumper 2. Here, A_P is the overall planform area.

et al. (1996) showed that the lift-to-drag ratio was increased as the body-ski angle decreased from 15° to −5° at the attack angle of skis of 30° and the hip angle of 164°. Schmölzer and Müller (2002) also showed that the lift-to-drag ratio was increased and drag and lift areas were decreased as the body-ski angle decreased from 15° to 0° at the attack angle of skis of 35.5° and hip angle of 160°. With the present flight postures obtained, the drag and lift areas on the legs were decreased with a significant increase of the lift-to-drag ratio, but those on the skis were increased with a slight increase of the lift-to-drag ratio, which resulted in overall decrease and increase of the total drag and lift areas, respectively. The decrease and increase of the total drag and lift areas, respectively, increased the flight distance according to Schmölzer and Müller (2002), Müller (2009), and Jung et al. (2014).

Limitations of our study: First, we did not consider the pitching moment in the present study. To obtain the pitching moment, the density distribution of a ski jumper and skis should be precisely known to locate the center of mass. Since the pitching moment is directly related with the flight stability, its variation with the flight posture is another important element to investigate. Second, we fix the attack angle of skis at 30° and varied other geometric angles to obtain a better flight posture for higher lift-to-drag ratio. In reality, this angle of attack continuously increases from 26° to 39° during the flight (Schmölzer and Müller, 2002). Combining temporal variation of the attack angle with the present procedure should provide a realistic estimation of the flight distance. Third, we did not consider the interaction between air and soft suit. Jung et al. (2014) showed that the drag

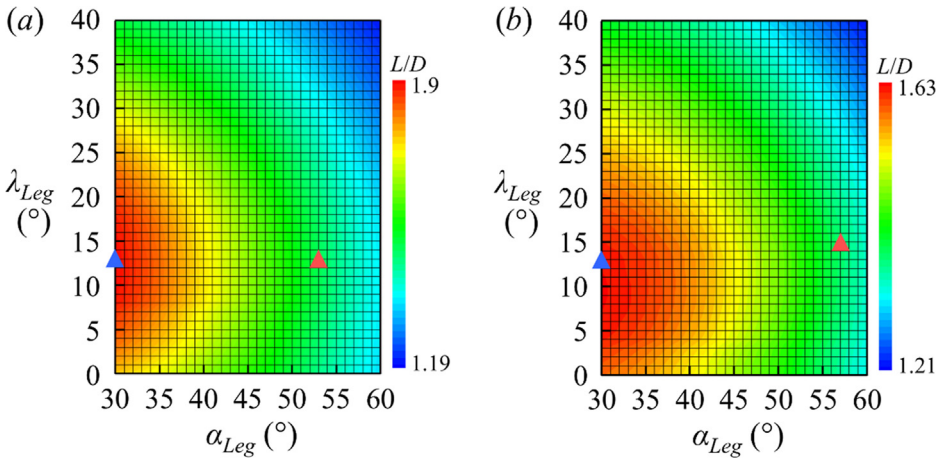

Fig. 5. Contours of the total lift-to-drag ratio with α_{Leg} (=$\alpha_{Right\ leg}$ = $\alpha_{Left\ leg}$) and λ_{Leg} (=$\lambda_{Right\ leg}$ = $\lambda_{Left\ leg}$) using the present geometric models: (a) jumper 1; (b) jumper 2. Blue triangles denote the postures of highest lift-to-drag ratios (red triangles indicate the base leg postures). (For interpretation of the references to colour in this figure legend, the reader is referred to the web version of this article.)

and lift areas were reduced as the suit became tight, which resulted in the decrease of the flight distance. Numerical simulation including this aspect is quite a challenging task.

5. Conclusions

In the present study, we suggested simple geometric models (cylinder, sphere and rectangular plate) to predict the drag and lift forces on each component (head, body, arms, legs and skis) of a flight posture. The predictions by the present models were in good agreements with those from LES. With these models, flight postures having higher lift-to-drag ratios were obtained and their performance was verified by LES. This indicated that the present geometric models are adequate for finding a flight posture of ski jumping having a higher lift-to-drag ratio at low cost. Nevertheless, the issues mentioned above (Limitations of our study) should be investigated further in the near future.

Conflict of interest statement

The authors declare that there is no conflict of interest regarding the content of this article.

Acknowledgments

This work was supported by the National Research Foundation through the Ministry of Science and ICT (No. NRF-2014M3C1B1033848). We are also grateful to national team members for providing their flight postures and to the KISTI Supercomputing Center for providing supercomputing resources and technical support (no. KSC-2015-C2-022).

Appendix A. Supplementary material

Supplementary data to this article can be found online at https://doi.org/10.1016/j.jbiomech.2019.04.022.

References

Bang, K., Kim, H., Choi, H., Ahn, E., Jeong, D., 2015. Flow characteristics of a ski jumper model. Proceedings of the ASME-JSME-KSME joint fluids engineering conference 2015. AJK2015-15306.
Blevins, R.D., 1984. Applied fluid dynamics handbook. Van Nostrand Reinhold Co, New York.
Gardan, N., Schneider, A., Polidori, G., Trenchard, H., Seigneur, J.M., Beaumont, F., Fourchet, F., Taiar, R., 2017. Numerical investigation of the early flight phase in ski-jumping. J. Biomech. 59, 29–34.
Jung, A., Staat, M., Müller, W., 2014. Flight style optimization in ski jumping on normal, large, and ski flying hills. J. Biomech. 47, 716–722.
Jung, A., Müller, W., Staat, M., 2018. Wind and fairness in ski jumping: A computer modelling analysis. J. Biomech. 75, 147–153.
Lee, K.-D., Park, M.-J., Kim, K.-Y., 2012. Optimization of ski jumper's posture considering lift-to-drag ratio and stability. J. Biomech. 45, 2125–2132.
Meile, W., Reisenberger, E., Mayer, M., Schmölzer, B., Müller, W., Brenn, G., 2006. Aerodynamics of ski jumping: experiments and CFD simulations. Exp. Fluids 41, 949–964.
Müller, W., 2009. Determinants of ski-jump performance and implications for health, safety and fairness. Sports Med. 39, 85–106.
Müller, W., Platzer, D., Schmölzer, B., 1995. Scientific approach to ski safety. Nature 375, 455.
Müller, W., Platzer, D., Schmölzer, B., 1996. Dynamics of human flight on skis: improvements in safety and fairness in ski jumping. J. Biomech. 29, 1061–1068.
Schmölzer, B., Müller, W., 2002. The importance of being light: aerodynamic forces and weight in ski jumping. J. Biomech. 35, 1059–1069.
Schmölzer, B., Müller, W., 2005. Individual flight styles in ski jumping: results obtained during Olympic Games competitions. J. Biomech. 38, 1055–1065.
Schwameder, H., 2008. Biomechanics research in ski jumping, 1991–2006. Sports Biomech. 7, 114–136.
Seo, K., Murakami, M., Yoshida, K., 2004. Optimal flight technique for V-style ski jumping. Sports Eng. 7, 97–103.
Yamamoto, K., Tsubokura, M., Ikeda, J., Onishi, K., Baleriola, S., 2016. Effect of posture on the aerodynamic characteristics during take-off in ski jumping. J. Biomech. 49, 3688–3696.
Yamanobe, K., Shirasaki, K., Akashi, K., Ishige, Y., 2016. The effects of upper limbs position on the aerodynamics in ski jumping flight. ISBS-Conference Proceedings Archive 34(1).